Inorg. Chem. **2005**, *44*, 4254–4262

Structural and Photophysical Properties of Lathanide(III) Complexes with a Novel Octadentate Iminophenolate Bibracchial Lariat Ether

Marina González-Lorenzo,[†] Carlos Platas-Iglesias,[†] Fernando Avecilla,[†] Stephen Faulkner,[‡] Simon J. A. Pope,[‡] Andrés de Blas,*[,†] and Teresa Rodríguez-Blas*[,†]

Departamento de Química Fundamental, Universidade da Coruña, Campus da Zapateira s/n 15071 A Coruña, Spain, and Department of Chemistry, University of Manchester, Oxford Road, Manchester M13 9PL, U.K.

Received December 27, 2004

We report here a structural and photophysical study of lanthanide complexes with the di-deprotonated form of the bibracchial lariat ether *N*,*N*′-bis(2-salicylaldiminobenzyl)-4,10-diaza-12-crown-4 (**L**^{3}) (Ln = Ho(III)–Lu(III)). The X-ray crystal structures of [Ho(**L**^{3}–2H)](ClO_4) (**1**) and [Er(**L**^{3}–2H)](ClO_4) (**2**) show the metal ion being eight-coordinate and deeply buried in the cavity of the dianionic receptor. Both sidearms of **L**^{3} are on the same side of the crown moiety, resulting in a syn conformation. Likewise, the lone pair of both pivotal nitrogen atoms is directed inward of the receptor cavity in an *endo*–*endo* arrangement and the coordination polyhedron around the lanthanide ion may be described as a distorted square antiprism that shows a deformation toward a square prism by ca. 11°. Attempts to isolate complexes of the lightest members of the lanthanide series were unsuccessful, which suggests a certain degree of selectivity of **L**^{3} toward the heaviest Ln(III) ions. This was evaluated and rationalized on the basis of theoretical calculations performed in vacuo at the HF level, by using the 3-21G* basis set for the ligand atoms and a 46+4f^{n} effective core potential for lanthanides. For the [Ln(**L**^{3}–2H)]$^{+}$ systems, the calculated bond distances between the metal ion and the coordinated donor atoms decrease along the lanthanide series, as usually observed for Ln(III) complexes. However, for the related [Ln(**L**^{1}–2H)]$^{+}$ and [Ln(**L**^{2}–2H)]$^{+}$ systems our ab initio calculations provide geometries in which some of the bond distances of the metal coordination environment increase across the lanthanide series. Thus, thanks to the variation of the ionic radii of the lanthanide ions, receptors **L**^{1} (*N*,*N*′-bis(2-salicylaldiminobenzyl)-4,13-diaza-18-crown-6) and **L**^{2} (*N*,*N*′-bis(2-salicylaldiminobenzyl)-1,10-diaza-15-crown-5) are specially adapted for the complexation of the lighter lanthanide ions. On the other hand, the erbium and ytterbium complexes of **L**^{3} have been shown to be emissive in the near-IR. Time-resolved studies of complexes confirm that solvent is excluded from the inner coordination sphere in solution. The luminescence properties of the complexes make them ideally suited for use as luminescent tags and suggest that $q = 0$ complexes of erbium may, after all, be useful as luminescent tags in protic media.

Introduction

The cyclic framework of crown ethers affords an interesting platform for the complexation of metal ions. The relative facility with which crown ethers can be functionalized with pendant arm(s) containing additional donor atom(s) allows one to enhance the cation binding ability and the selectivity of the parent crown ether.[1,2] In particular, the hard acid character of the crown moiety makes crown ethers interesting potential ligands for the complexation of trivalent lanthanide ions,[3] including the design of efficient lanthanide-based luminescent devices. A unique combination of features must be realized to design a lanthanide luminescence sensor: (i) presence of multiple absorbing groups suitable for energy transfer (antenna effect[4]), (ii) high thermodynamic and kinetic inertness, and (iii) protection of the metal ion from various quenching or back-transfer processes.[5,6] The intense, long-lived emission from Eu(III) and Tb(III) has made their

* Corresponding authors. Fax: (+34) 981-16-70-65. E-mail: mayter@udc.es (T.R.-B); ucambv@udc.es (A.B.).
[†] Universidade da Coruña.
[‡] University of Manchester.

(1) Gokel, G. W.; Korzeniowski, S. H. *Macrocyclic Polyether Synthesis*; Springer: Berlin, 1982.
(2) Nakatsuji, Y.; Nakamura, T.; Yometani, M.; Yuya, H.; Okahara, M. *J. Am. Chem. Soc*. **1988**, *110*, 531.
(3) Liu, Y.; Han, B.-H.; Li, Y.-M.; Chen, R.-T.; Ouchi, M.; Inoue, Y. *J. Chem. Phys*. **1996**, *100*, 17361.

10.1021/ic048172a CCC: $30.25
Published on Web 05/14/2005

Chart 1

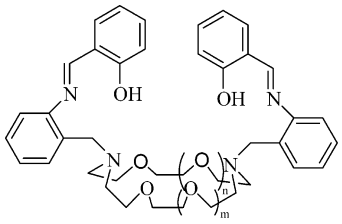

L^1: n = 1, m = 1
L^2: n = 1, m = 0
L^3: n = 0, m = 0

compounds of great interest as luminescence sensors[7] or as probes for sensitive homogeneous fluoroimmunoassays.[8] In contrast, the longer wavelength luminescence from other lanthanides such as Nd(III), Er(III), and Yb(III) has only recently become of interest.[9] Several different approaches have been developed to sensitize near-infrared emission from Yb(III), Nd(III), or Er(III) complexes, including the use of transition metal based antenna groups[9] or organic chromophores. In addition, Schiff-base macrocyclic receptors have also turned out to be good candidates for the sensitization of Yb(III) and Nd(III) ions because the electronic delocalization in the ligand induces a relatively low lying triplet state that provides an efficient conversion of the visible light absorbed into near-infrared light emitted by these ions.[10,11]

In recent work, we described the coordinative ability toward lanthanide(III) ions of two di-deprotonated lariat ethers containing salicylaldimino-benzyl pendant arms and derived from 4,13-diaza-18-crown-6 (**L**^{1})[12] or 1,10-diaza-15-crown-5 (**L**^{2})[13] (Chart 1). In these studies we demonstrated that **L**^{1} forms stable complexes in acetonitrile solution only with the three lightest lanthanide ions (La, Ce, and Pr), as a consequence of the combination of the relatively large ring size of the crown moiety and the presence of relatively rigid pendant arms. However, the smaller ring size of **L**^{2} allows one to obtain stable complexes with the Ln(III) ions from La(III) to Ho(III). Herein, we present the synthesis and the structural characterization of lanthanide complexes with formula [Ln(**L**^{3}−2H)](ClO_4), Ln = Ho−Lu, where **L**^{3} is the lariat ether *N*,*N*′-bis(2-salicylaldiminobenzyl)-4,10-diaza-12-crown-4. The crystal structures of the Ho(III) and Er(III) complexes were determined by X-ray crystallography. ^{1}H and ^{13}C NMR spectroscopy has been used to obtain structural information on the Ln(III) complexes in acetonitrile solution. The complexes were also characterized by ab initio calculations at the HF/3-21G* level. Calculated molecular geometries and ^{13}C NMR spectra are compared with the experimental values. The photophysical properties of the Er(III), Yb(III), and Lu(III) complexes are also reported.

Experimental Section

Materials. Lanthanide(III) perchlorate hydrates were purchased from Alfa laboratories and used as received. All other chemicals were purchased from commercial sources and used without further purification. Solvents were of reagent grade and were purified by the usual methods. Acetonitrile-d_3 for NMR measurements (Merck, 99% D) was used as received.

CAUTION! Perchlorate salts combined with organic ligands are potentially explosive and should be handled in small quantities and with the necessary precautions.[14]

Synthesis. *N*,*N*′-Bis(2-aminobenzyl)-4,10-diaza-12-crown-4. A solution of 2-nitrobenzyl chloride (1.000 g, 5.828 mmol) in acetonitrile (20 mL) was added to a refluxing mixture of 4,10-diaza-12-crown-4 (0.500 g, 2.869 mmol) and Na_2CO_3 (1.520 g, 14.339 mmol) in the same solvent (30 mL). The reaction mixture was stirred under reflux for 24 h. It was then filtered, the filtrate was concentrated, and the yellow oily residue was extracted with CH_2Cl_2/water. The organic phase was dried with anhydrous $MgSO_4$ and concentrated in vacuo to give a brown oil corresponding to the intermediate *N*,*N*′-bis(2-nitrobenzyl)-4,10-diaza-12-crown-4. δ_H (solvent $CDCl_3$; standard $SiMe_4$): 8.02 (d, 2H, arH, ^3J = 7.81 Hz), 7.88 (d, 2H, arH, ^3J = 8.30 Hz), 7.60 (td, 2H, arH, ^3J = 7.81 Hz, ^4J = 1.46 Hz), 7.39 (td, 2H, arH, ^3J = 8.30 Hz, ^4J = 1.95 Hz), 3.98 (s, 4H, N−CH_2−ar), 3.58 (t, 8H, −O−CH_2−, ^3J = 4.89 Hz), 2.75 (t, 8H, N−CH_2−, ^3J = 4.88 Hz). This oil was dissolved in ethanol (60 mL) and heated to reflux. Hydrazine hydrate (1.0 mL) was added, and then the reaction mixture was heated and stirred for 20 min. It was then filtered, and the solvent was removed from the filtrate in a rotary evaporator. Addition of cold diethyl ether to the oily residue led to the deposition of a white precipitate, which was collected by filtration (yield 0.55 g, 50%). Anal. Calcd for $C_{22}H_{32}N_4O_2 \cdot H_2O$: C, 65.6; H, 8.5; N, 14.1%. Found: C, 65.6; H, 8.2; N, 14.1%. FAB-MS [*m*/*z* (% BPI)]: 385 (40%) $[M + H]^+$. IR (KBr): $\nu(NH_2)$ 3430, 3318, $\delta(NH_2)$ 1611 cm^{-1}. δ_H (solvent $CDCl_3$; standard $SiMe_4$): 7.10 (td, 2H, arH, ^3J = 7.33 Hz, ^4J = 1.47 Hz), 6.97 (d, 2H, arH, ^3J = 7.33 Hz), 6.65 (m, 4H, arH), 4.90 (b, 4H, $-NH_2$), 3.61 (s, 4H, N−CH_2−ar), 3.48 (t, 8H, −O−CH_2−, ^3J = 4.88 Hz), 2.71 (t, 8H, N−CH_2-, ^3J = 4.89 Hz).

Preparation of the Complexes. *N*,*N*′-Bis(2-aminobenzyl)-4,10-diaza-12-crown-4 (0.050 g, 0.130 mmol) and 0.044 g of salicylaldehyde (0.260 mmol) were dissolved in 2-propanol (30 mL) and heated to reflux. After 1 h a solution of 0.026 g of triethylamine (0.260 mmol) in 10 mL of 2-propanol was added, and the reflux was maintained for 30 min. A solution of the corresponding hydrated lanthanide(III) perchlorate (0.130 mmol) in 25 mL of the same solvent was then added, the resultant solution was refluxed for 3 h and filtered while hot, and the filtrate was left to evaporate slowly at room temperature to yield yellow crystals, which were collected by filtration and dried under vacuum over $CaCl_2$.

[Ho(L^{3}−2H)](ClO_4) (1). Yield: 0.095 g, 85%. Anal. Calcd for $C_{36}H_{38}ClHoN_4O_8$: C, 50.6; H, 4.5; N, 6.6%. Found: C, 50.6; H,

(4) Sabbatini, N.; Perathoner, S.; Balzani, V.; Alpha, B.; Lehn, J.-M. In *Supramolecular Chemistry*; Balzani, V., Ed.; Reidel Publishing Co.: Dordrecht, 1987.
(5) Blasse, G. *Phys. Status Solidi A* **1992**, *130*, K85.
(6) Bünzli, J.-C. G.; Froidevaux, P.; Harrowfield, J. M. *Inorg. Chem.* **1993**, *32*, 3306.
(7) Parker, D. *Coord. Chem. Rev.* **2000**, *205*, 109.
(8) Yam, V. W. W.; Lo, K. K. W. *Coord. Chem. Rev.* **1999**, *184*, 157.
(9) Shavaleev, N. M.; Moorcraft, L. P.; Pope, S. J.; Bell, Z. R.; Faulkner, S.; Ward, M. D. *Chem. Eur. J.* **2003**, *9*, 5283.
(10) Platas, C.; Avecilla, F.; de Blas, A.; Rodríguez-Blas, T.; Geraldes, C. F. G. C.; Tóth, É.; Merbach, A. E.; Bünzli, J.-C. G. *J. Chem. Soc., Dalton Trans.* **2000**, 611.
(11) Rodríguez-Cortiñas, R.; Avecilla, F.; Platas-Iglesias, C.; Imbert, D.; Bünzli, J.-C. G.; de Blas, A.; Rodríguez-Blas, T. *Inorg. Chem.* **2002**, *41*, 5336.
(12) Platas, C.; Avecilla, F.; de Blas, A.; Rodríguez-Blas, T.; Bastida, R.; Macías, A.; Rodríguez, A.; Adams, H. *J. Chem. Soc., Dalton Trans.* **2001**, 1699.
(13) González-Lorenzo, M.; Platas-Iglesias, C.; Avecilla, F.; Geraldes, C. F. G. C.; Imbert, D.; Bünzli, J.-C. G.; de Blas, A.; Rodríguez-Blas, T. *Inorg. Chem.* **2003**, *42*, 6946.
(14) Wolsey, W. C. *J. Chem. Educ.* **1973**, *50*, A335.

4.4; N, 6.6%. FAB-MS [*m*/*z* (% BPI)]: 755 (100%) [Ho(**L**^{3}−2H)]$^+$. IR (KBr): (C═N) 1608, (C═C) 1536, (ClO_4^-) 1078 and 623 cm^{-1}. Yellow single crystals of **1**, suitable for single-crystal X-ray diffraction analysis, were grown by slow evaporation of 2-propanol solutions of the complex.

[Er(L^3−2H)](ClO$_4$)·H$_2$O (2). Yield: 0.102 g, 90%. Anal. Calcd for $C_{36}H_{38}ClErN_4O_8 \cdot H_2O$: C, 49.4; H, 4.6; N, 6.4%. Found: C, 49.6; H, 4.5; N, 6.5%. FAB-MS [*m*/*z* (% BPI)]: 758 (100%) [Er(**L**^{3}−2H)]$^+$. IR (KBr): (C═N) 1608, (C═C) 1537, (ClO_4^-) 1076 and 623 cm^{-1}. Yellow single crystals of **2**, suitable for single-crystal X-ray diffraction analysis, were grown by slow evaporation of 2-propanol solutions of the complex.

[Tm(L^3−2H)](ClO$_4$)·1.5H$_2$O (3). Yield: 0.098 g, 86%. Anal. Calcd for $C_{36}H_{38}ClN_4O_8Tm \cdot 1.5H_2O$: C, 48.7; H, 4.6; N, 6.3%. Found: C, 48.8; H, 4.2; N, 6.0%. FAB-MS [*m*/*z* (% BPI)]: 759 (100%) [Tm(**L**^{3}−2H)]$^+$. IR (KBr): (C═N) 1608, (C═C) 1537, (ClO_4^-) 1075 and 623 cm^{-1}.

[Yb(L^3−2H)](ClO$_4$)·H$_2$O (4). Yield: 0.110 g, 96%. Anal. Calcd for $C_{36}H_{38}ClN_4O_8Yb \cdot H_2O$ C, 49.1; H, 4.6; N, 6.4%. Found: C, 49.0; H, 4.4; N, 6.4%. FAB-MS [*m*/*z* (% BPI)]: 764 (100%) [Yb(**L**^{3}−2H)]$^+$. IR (KBr): (C═N) 1608, (C═C) 1537, (ClO_4^-) 1074 and 622 cm^{-1}.

[Lu(L^3−2H)](ClO$_4$)·H$_2$O (5). Yield: 0.110 g, 96%. Anal. Calcd for $C_{36}H_{38}ClLuN_4O_8 \cdot H_2O$: C, 49.0; H, 4.6; N, 6.3%. Found: C, 48.9; H, 4.7; N, 6.5%.]. FAB-MS [*m*/*z* (% BPI)]: 765 (100%) [Lu(**L**^{3}−2H)]$^+$. IR (KBr): (C═N) 1611, (C═C) 1537, (ClO_4^-) 1091 and 623 cm^{-1}.

Measurements. Elemental analyses were carried out on a Carlo Erba 1108 elemental analyzer. FAB mass spectra were recorded using a FISONS QUATRO mass spectrometer with Cs ion gun and 3-nitrobenzyl alcohol matrix. ^{1}H and ^{13}C NMR spectra were run at 25 °C with Bruker AC200 F and Bruker WM-500 spectrometers. Chemical shifts are reported in parts per million with respect to TMS. Spectral assignments were based in part on two-dimensional COSY, HMQC, and HMBC experiments. IR spectra were recorded, as KBr disks, using a Bruker Vector 22 spectrophotometer. Electronic spectra in the UV−vis range were recorded at 20 °C on a Perkin-Elmer Lambda 900 UV−vis spectrophotometer using 1.0 cm quartz cells. Photophysical studies (steady-state and time-resolved luminescence) were carried out by using instrumentation and methods described elsewhere.[15] Luminescence lifetimes were obtained by iterative reconvolution of the detector response with components for growth and decay of the metal centered emission.[15] In all cases, good fits were obtained for a single-exponential decay.

X-ray Data Collections and Structure Determinations. Crystal data and details on data collection and refinement are summarized in Table 1. Three-dimensional, room temperature X-ray data were collected in the θ range 0.90° to 28.28° (**1**) and 0.904° to 28.29° (**2**) on a Bruker Smart 1000 CCD instrument. Reflections were measured from a hemisphere of data collected from frames, each of them covering 0.3° in ω. Of the 10 985 (**1**) and 11 038 (**2**) reflections measured, all of which were corrected for Lorentz and polarization effects and for absorption by semiempirical methods based on symmetry-equivalent and repeated reflections, 4408 (**1**) and 6036 (**2**) independent reflections exceeded the significance level ($|F|/\sigma|F|$) > 4.0. The structures were solved by direct methods and refined by full matrix least-squares on F^2. Hydrogen atoms were included in calculated positions and refined in the riding mode. Refinement was performed with allowance for thermal anisotropy of all non-hydrogen atoms. Minimum and maximum final electronic densities of −1.424 and 1.182 e Å^{-3} for **1** and −1.205 and 1.507 e Å^{-3} for **2** were found. Both structures present a disorder on perchlorate anion. These disorders have been resolved and two atomic sites have been observed for O(7) and O(8) in **1** and for O(8) in **2** and refined with anisotropic displacement parameters in each case. The site occupancy factors were 0.240(16) for O(7A) and O(8A) in **1** and 0.74(3) for O(8A) in **2**. Complex scattering factors were taken from the program package SHELXTL[16] as implemented on a Pentium computer.

Table 1. Crystal Data and Structure Refinement for **1** and **2**

	1	**2**
formula	$C_{36}H_{38}ClHoN_4O_8$	$C_{36}H_{38}ClErN_4O_8$
MW	855.08	857.41
crystal system	Triclinic	Triclinic
space group	$P\bar{1}$	$P\bar{1}$
T/K	293(2)	293(2)
a/Å	10.7121(14)	10.6968(7)
b/Å	12.1669(16)	12.1669(8)
c/Å	13.8915(18)	13.8704(10)
α/deg	84.123(2)	84.2090(10)
β/deg	77.422(2)	77.3940(10)
γ/deg	83.067(2)	83.1820(10)
V/Å^3	1748.7(4)	1744.0(2)
F_{000}	860	862
Z	2	2
D_{calc}/g cm^{-3}	1.624	1.633
μ/mm^{-1}	2.396	2.541
R_{int}	0.0469	0.0256
reflns measd	10985	11038
reflns obsd	4408	6036
GOF on F^2	0.987	1.037
R_1[a]	0.0623	0.0412
wR_2 (all data)[b]	0.1308	0.0976

[a] $R_1 = \sum||F_o| - |F_c||/\sum|F_o|$. [b] $wR_2 = \{\sum[w(|F_o|^2 - |F_c|^2)^2]|/\sum[w(F_o^4)]\}^{1/2}$.

Computational Methods. Full geometry optimizations of the [Ln(**L**^{3}−2H)]$^+$ systems (Ln = Ce, Sm, Ho−Lu) were performed in vacuo at the RHF and DFT (B3LYP functional)[17,18] levels. For these calculations the effective core potential (ECP) of Dolg et al. and the related [5s4p3d]-GTO valence basis set were used for the lanthanides,[19] while the 3-21G* basis set was used for the ligand atoms. Analogous calculations were also performed on the [Ln(**L**^{1}−2H)]$^+$ and [Ln(**L**^{2}−2H)]$^+$ systems (Ln = Ce, Sm, Ho, Lu). When available, the X-ray structures were used as input geometries. To avoid SCF convergence problems, a quadratic convergence procedure has been applied during the geometry optimizations. The nature of the calculated stationary points as true minima was checked by frequency analysis. The NMR shielding tensors of the [Lu(**L**^{3}−2H)]$^+$ system (GIAO[20] method) were calculated in vacuo at the DFT (B3LYP functional) level by using the ECP of Stevens et al.[21] and the 6-31G** basis set for the ligand atoms.[22] For chemical shift calculation purposes, NMR shielding tensors of tetramethylsilane (TMS) were calculated at the appropriate level. All HF and DFT calculations were performed by using the Gaussian 98 package (revision A.11.3).[23]

(15) Shavaleev, N. M.; Pope, S. J. A.; Bell, Z. R.; Faulkner, S.; Ward, M. D. *J. Chem. Soc., Dalton Trans*. **2003**, 808.
(16) Sheldrick. G. M. *SHELXTL*, release 5.1; Bruker Analytical X-ray System: Madison, WI 1997.
(17) Becke, A. D. *J. Chem. Phys*. **1993**, *98*, 5648.
(18) Lee, C.; Yang, W.; Parr, R. G. *Phys. Rev. B* **1988**, *37*, 785.
(19) Dolg, M.; Stoll, H.; Savin, A.; Preuss, H. *Theor. Chim. Acta* **1989**, *75*, 173.
(20) Ditchfield, R. *Mol. Phys*. **1974**, *27*, 789.
(21) Cundari, T. R.; Stevens, W. J. *J. Chem. Phys.* **1993**, *98*, 5555.
(22) A description of the basis sets and theory level used in this work can be found in the following: Foresman, J. B.; Frisch, A. E. *Exploring Chemistry with Electronic Structure Methods*, 2nd ed.; Gaussian Inc.: Pittsburgh, PA, 1996.

Results and Discussion

Synthesis and Characterization of the Complexes. Reaction of **L³** [prepared in situ by the condensation of *N*,*N*′-bis(2-aminobenzyl)-4,10-diaza-12-crown-4 and salicylaldehyde] with triethylamine and the corresponding hydrated lanthanide perchlorate in 2-propanol led to complexes of formula $[Ln(\mathbf{L^3}-2H)](ClO_4)\cdot xH_2O$ (Ln = Ho−Lu) in high yield (85−96%). Attempts to prepare the corresponding complexes of the lighter Ln(III) ions (Ln = La−Dy) by using analogous conditions were unsuccessful. In previous studies we demonstrated that **L¹** forms stable complexes in acetonitrile solution only with the three lightest lanthanide ions (La, Ce, and Pr), as a consequence of the combination of the relatively large ring size of the crown moiety and the presence of relatively rigid pendant arms. We also reported that the smaller ring size of **L²** allows one to obtain stable complexes with the Ln(III) ions from La(III) to Ho(III). The results presented here suggest a certain degree of selectivity of **L³** toward the heaviest Ln(III) ions (Ln = Ho−Lu). The IR and FAB-mass spectra of the complexes confirmed the formation of the Schiff-base lariat ether and its presence in the complexes. The IR spectra (KBr disks) feature a band attributable to the $\nu(C{=}N)_{imine}$ stretching mode at ca. 1608 cm^{-1}. The presence of this band together with the absence of bands due to carbonyl and/or amine vibration modes confirms the formation of the imine. Bands corresponding to the $\nu_{as}(Cl-O)$ stretching and $\delta_{as}(O-Cl-O)$ bending modes of the perchlorate groups appear at ca. 1100 and 630 cm^{-1}.[24] The absorption at 630 cm^{-1} clearly shows up without splitting, as befits an uncoordinated anion. The FAB-mass spectrum of each complex displays a very intense peak (100% BPI) corresponding to the $[Ln(\mathbf{L^3}-2H)]^+$ fragment.

The ^1H and ^{13}C NMR spectra of the Lu(III) diamagnetic complex **5** were recorded in acetonitrile-d_3 solution and assigned on the basis of two-dimensional COSY, HMQC, and HMBC experiments at 298 K (Table 2, see Figure 1 for the numbering scheme). The ^1H NMR spectrum is shown in Figure 1. Both the ^1H and ^{13}C NMR spectra agree with an effective C_2 symmetry of the complex in acetonitrile solution, the ^{13}C NMR spectrum showing 18 peaks for the 36 carbon atoms of the ligand backbone. The ^1H NMR spectrum shows a signal attributable to the H2 protons at unusually low frequency (5.54 ppm, Figure 1). Inspection of the X-ray structures of compounds **1** and **2** shows that these protons are directed toward the aromatic ring current of the phenol ring of the neighbor pendant arm. The large low-frequency shift observed for H2 protons is therefore attributable to a ring current shift effect provoked by the phenol rings, which results in a shielding for any nuclei above or below this ring. Since assignments to specific axial/equatorial CH_2 protons were not possible on the basis of the 2D NMR spectra, they were carried out using the stereochemically dependent proton shift effects, resulting from the polarization of the C−H

Table 2. ^1H and ^{13}C NMR Shifts (δ/ppm, with Respect to TMS) for the $[Lu(\mathbf{L^3}-2H)]^+$ Complex[a]

^1H	$\delta_{i,exp}$[b]	^{13}C	$\delta_{i,exp}$[b]	$\delta_{i,calc}$[c]
H2	5.54	C1	166.7	181.0
H3	7.08	C2	120.8	111.9
H4	6.53	C3	135.3	134.0
H5	7.26	C4	114.9	115.7
H7	8.17	C5	135.4	134.2
H9	6.51	C6	121.9	119.7
H10	7.18	C7	169.2	166.6
H11	7.24	C8	154.8	151.9
H12	7.38	C9	121.8	122.3
H14a	3.26	C10	130.3	129.2
H14b	4.30	C11	125.6	123.1
$H15_{ax}$	2.51	C12	130.9	127.4
$H15_{eq}$	3.38	C13	127.9	124.7
$H16_{ax}$	3.63	C14	59.4	62.4
$H16_{eq}$	4.10	C15	54.3	50.3
$H17_{ax}$	3.95	C16	69.0	60.8
$H17_{eq}$	4.03	C17	69.2	60.3
$H18_{ax}$	2.52	C18	51.8	49.2
$H18_{eq}$	3.95			

[a] See Figure 1 for labeling scheme. [b] Conditions: Assignment supported by 2D H,H COSY, HMQC, and HMBC experiments at 293 K, CD_3CN, 500 MHz. $^3J_{2-3} = 8.5$ Hz; $^4J_{3-5} = {}^4J_{5-3} = 1.5$ Hz; $^3J_{9-10} = 7.4$ Hz; $^3J_{12-11} = 7.1$ Hz; $^2J_{14a-14b} = {}^2J_{14b-14a} = 12.7$ Hz. [c] Values calculated in vacuo at the B3LYP/6-31G** level by using the GIAO method.

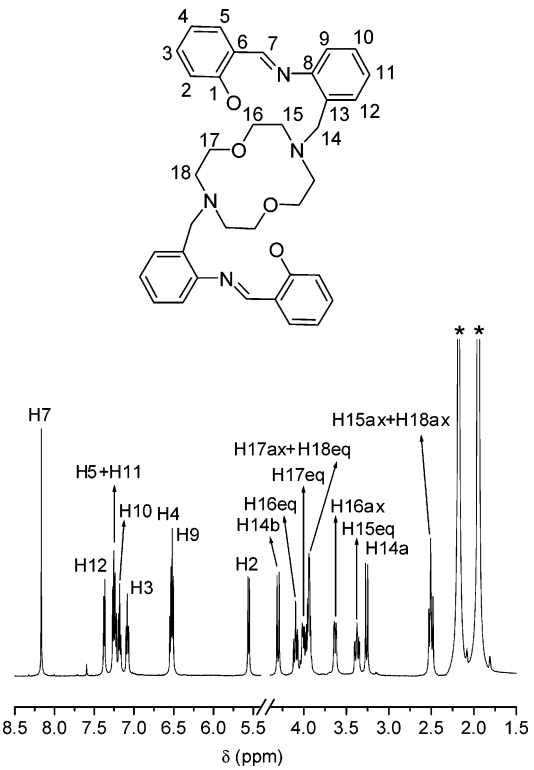

Figure 1. The 500 MHz ^1H NMR spectrum of the Lu(III) complex **5** as recorded in acetonitrile-d_3 solution at 293 K. Solvent signals are denoted with an asterisk.

(23) Frisch, M. J.; Trucks, G. W.; Schlegel, H. B.; Scuseria, G. E.; Robb, M. A.; Cheeseman, J. R.; Zakrzewski, V. G.; Montgomery, J. A., Jr.; Stratmann, R. E.; Burant, J. C.; Dapprich, S.; Millam, J. M.; Daniels, A. D.; Kudin, K. N.; Strain, M. C.; Farkas, O.; Tomasi, J.; Barone, V.; Cossi, M.; Cammi, R.; Mennucci, B.; Pomelli, C.; Adamo, C.; Clifford, S.; Ochterski, J.; Petersson, G. A.; Ayala, P. Y.; Morokuma, K. Cui, Q.; Malick, D. K.; Rabuck, A. D.; Raghavachari, K.; Foresman, J. B.; Cioslowski, J.; Ortiz, J. V.; Baboul, A. G.; Stefanov, B. B.; Liashenko, G. Liu, A.; Piskorz, P.; Komaromi, I.; Gomperts, R.; Martin, R. L.; Fox, D. J.; Keith, T.; Al-Laham, M. A.; Peng, C. Y.; Nanayakkara, A.; Challacombe, M.; Gill, P. M. W.; Johnson, B.; Chen, W.; Wong, M. W.; Andres, J. L.; Gonzalez, C.; Head-Gordon, M.; Replogle, E. S.; Pople, J. A. *Gaussian 98*, revision A.11; Gaussian, Inc.: Pittsburgh, PA, 1998.

(24) Nakamoto, K. *Infrared and Raman Spectra of Inorganic and Coordination Compounds*, 3rd ed.; J. Wiley: New York, Chichester, Brisbane, and Toronto, 1972; pp 142−154.

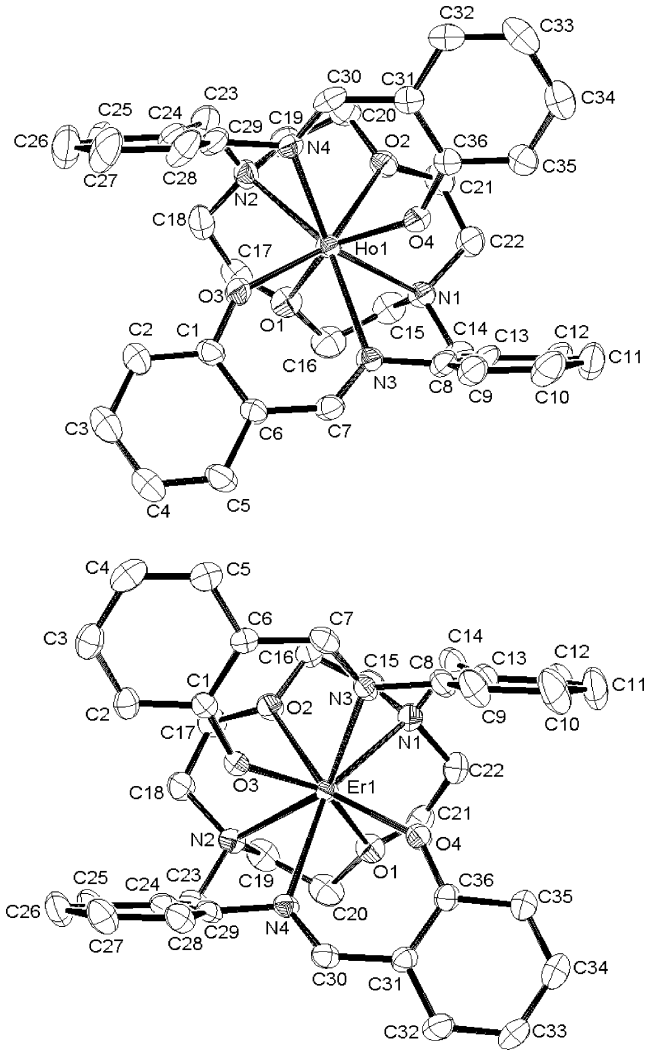

Figure 2. Crystal structures of $[Ho(\mathbf{L^3}-2H)]^+$ (top, $\Lambda(\delta\delta\delta\delta)$ isomer) and $[Er(\mathbf{L^3}-2H)]^+$ (bottom, $\Delta(\lambda\lambda\lambda\lambda)$ isomer). Hydrogen atoms are omitted for simplicity. The ORTEP plots are at the 30% probability level.

bonds by the electric field generated by the cation charge,[25] as predicted from the X-ray crystal structure of **2**. This polarization results in a deshielding of the equatorial and the H14b protons, which are pointing away from the metal ion.

X-ray Crystal Structures of 1 and 2. The solid-state structures of compounds $[Ho(\mathbf{L^3}-2H)](ClO_4)$ (**1**) and $[Er(\mathbf{L^3}-2H)](ClO_4)$ (**2**) have been determined by X-ray diffraction studies. Crystals of **1** and **2** consist of $[Ho(\mathbf{L^3}-2H)]^+$ and $[Er(\mathbf{L^3}-2H)]^+$ cations, respectively, and one well-separated perchlorate anion. Both complexes crystallize in the triclinic space group $P\bar{1}$, and they are isostructural. In both cations the corresponding lanthanide ion is bound to the eight available donor atoms of the bibracchial lariat ether as shown in Figure 2. Table 3 summarizes selected bond lengths and angles of the lanthanide coordination sphere in **1** and **2**. All bond distances of the metal ion coordination sphere are standard.[26−28] Figure 2 allows an appraisal of the conformation adopted by the bibracchial lariat ether in **1** and **2**. Both sidearms are on the same side of the crown moiety, resulting in a syn conformation. Likewise, the lone pair of both pivotal nitrogen atoms is

Table 3. Selected Bond Lengths (Å) and Angles (deg) for **1** and **2**

	$[Ho(\mathbf{L^3}-2H)](ClO_4)$ (**1**)		
Ho(1)−O(1)	2.443(6)	Ho(1)−N(1)	2.666(6)
Ho(1)−O(2)	2.445(5)	Ho(1)−N(2)	2.641(7)
Ho(1)−O(3)	2.156(5)	Ho(1)−N(3)	2.542(6)
Ho(1)−O(4)	2.157(5)	Ho(1)−N(4)	2.478(6)
O(3)−Ho(1)−O(4)	118.3(2)	N(4)−Ho(1)−N(3)	119.41(19)
O(3)−Ho(1)−O(1)	82.3(2)	O(3)−Ho(1)−N(2)	86.90(19)
O(4)−Ho(1)−O(1)	149.1(2)	O(4)−Ho(1)−N(2)	132.45(19)
O(3)−Ho(1)−O(2)	153.28(19)	O(1)−Ho(1)−N(2)	66.7(2)
O(4)−Ho(1)−O(2)	78.90(18)	O(2)−Ho(1)−N(2)	66.99(18)
O(1)−Ho(1)−O(2)	91.92(19)	N(4)−Ho(1)−N(2)	72.5(2)
O(3)−Ho(1)−N(4)	80.1(2)	N(3)−Ho(1)−N(2)	153.7(2)
O(4)−Ho(1)−N(4)	73.23(19)	O(3)−Ho(1)−N(1)	132.65(19)
O(1)−Ho(1)−N(4)	136.2(2)	O(4)−Ho(1)−N(1)	82.96(19)
O(2)−Ho(1)−N(4)	86.38(18)	O(1)−Ho(1)−N(1)	66.5(2)
O(3)−Ho(1)−N(3)	73.44(19)	O(2)−Ho(1)−N(1)	65.91(18)
O(4)−Ho(1)−N(3)	73.38(19)	N(4)−Ho(1)−N(1)	146.6(2)
O(1)−Ho(1)−N(3)	93.0(2)	N(3)−Ho(1)−N(1)	73.69(18)
O(2)−Ho(1)−N(3)	133.12(18)	N(2)−Ho(1)−N(1)	110.0(2)
	$[Er(\mathbf{L^3}-2H)](ClO_4)$ (**2**)		
Er(1)−O(1)	2.436(4)	Er(1)−N(1)	2.644(4)
Er(1)−O(2)	2.438(3)	Er(1)−N(2)	2.644(4)
Er(1)−O(3)	2.143(3)	Er(1)−N(3)	2.482(4)
Er(1)−O(4)	2.139(4)	Er(1)−N(4)	2.519(4)
O(4)−Er(1)−O(3)	118.13(14)	N(3)−Er(1)−N(4)	119.07(13)
O(4)−Er(1)−O(2)	153.05(12)	O(4)−Er(1)−N(1)	87.10(13)
O(3)−Er(1)−O(2)	79.14(13)	O(3)−Er(1)−N(1)	132.67(13)
O(4)−Er(1)−O(1)	82.13(14)	O(2)−Er(1)−N(1)	66.61(12)
O(3)−Er(1)−O(1)	149.30(13)	O(1)−Er(1)−N(1)	66.34(13)
O(2)−Er(1)−O(1)	92.09(13)	N(3)−Er(1)−N(1)	73.23(14)
O(4)−Er(1)−N(3)	79.81(14)	N(4)−Er(1)−N(1)	153.39(14)
O(3)−Er(1)−N(3)	73.10(12)	O(4)−Er(1)−N(2)	132.83(13)
O(2)−Er(1)−N(3)	86.64(13)	O(3)−Er(1)−N(2)	82.76(13)
O(1)−Er(1)−N(3)	136.25(13)	O(2)−Er(1)−N(2)	66.07(12)
O(4)−Er(1)−N(4)	73.20(13)	O(1)−Er(1)−N(2)	66.90(13)
O(3)−Er(1)−N(4)	73.60(14)	N(3)−Er(1)−N(2)	146.62(14)
O(2)−Er(1)−N(4)	133.60(13)	N(4)−Er(1)−N(2)	73.68(12)
O(1)−Er(1)−N(4)	92.76(13)	N(1)−Er(1)−N(2)	109.80(13)

directed inward of the receptor cavity in an *endo*−*endo* arrangement. The coordination polyhedron around the lanthanide ion may be described as a distorted square antiprism composed of two parallel pseudoplanes (see Figure 2): O(3), O(4), N(3), and N(4) define the upper pseudoplane (mean deviation from planarity 0.0885 Å for **1** and 0.0857 Å for **2**) while O(1), O(2), N(1), and N(2) define the lower pseudoplane (mean deviation from planarity 0.0797 (**1**) and 0.0833 Å (**2**)). The angle between these two least-squares planes amounts to 3.3° (**1**) and 2.6° (**2**), the lanthanide ion being placed at 1.1832 (**1**) and 1.1819 (**2**) Å from the upper plane and 1.6105 (**1**) and 1.6058 (**2**) Å from plane formed by O(1), O(2), N(1), and N(2). The twist angle, ω,[29] between these nearly parallel squares is 33.9° (**1**) and 34.1° (**2**), showing a deformation of the coordination polyhedron from a square antiprism (ideal value 45°) toward a square prism (ideal value 0°) by ca. 11°.

The square-antiprismatic geometry of $[Ln(\mathbf{L^3}-2H)]^+$ complexes implies the occurrence of two helicities (one

(25) Harris, R. K. *Nuclear Magnetic Resonance Spectroscopy: A Physicochemical View*; Pitman: London, 1983.
(26) Dickins, R. S.; Loue, C. S.; Puschmann, H. *Chem. Commun.* **2001**, 2308.
(27) Rogers, R. D.; Rollins, A. N.; Benning, M. M. *Inorg. Chem.* **1988**, *27*, 3826.
(28) Kanesato, M.; Vokoyama, T. *Chem. Lett.* **1999**, 241.
(29) Piguet, C.; Bünzli, J.-C. G.; Bernardinelli, G.; Bochet C. G.; Froidevaux, P. *J. Chem. Soc., Dalton Trans.* **1995**, 83.

belonging to the crown moiety and one associated with the layout of the pendant arms), which may give rise to two enantiomeric pairs of diastereoisomers.[30,31] Inspection of the crystal structure data reveals that in **1** and **2** two $\Lambda(\delta\delta\delta\delta)$ and $\Delta(\lambda\lambda\lambda\lambda)$ enantiomers cocrystallize in equal amounts (racemate).

Ab Initio Calculations. The $[Ln(\mathbf{L^3}-2H)]^+$ systems (Ln = Ce, Sm, Ho−Lu) were investigated in vacuo by means of ab initio calculations at the HF level. As there is not a good all-electron basis set for lanthanides, the effective core potential (ECP) of Dolg et al. and the related [5s4p3d]-GTO valence basis set were applied in these calculations.[19] This ECP includes $46+4f^n$ electrons in the core, leaving the outermost 11 electrons to be treated explicitly, and it has been demonstrated to provide reliable results for the lanthanide aqua ions,[32] several lanthanide complexes with polyamino carboxylate ligands,[33,34] and lanthanide dipicolinates.[35] Compared to all-electron basis sets, ECPs account to some extent for relativistic effects, which are believed to become important for the elements from the fourth row of the periodic table. In vacuo optimized Cartesian coordinates obtained for the different $[Ln(\mathbf{L^3}-2H)]^+$ (Ln = Ho−Lu) systems are given in the Supporting Information. The calculated structures of the $[Ho(\mathbf{L^3}-2H)]^+$ and $[Er(\mathbf{L^3}-2H)]^+$ systems are in good agreement with the experimental geometrical parameters obtained from the X-ray analysis of compounds **1** and **2** (Table 4). Our calculations overestimate the distances between the lanthanide ion and the oxygen atoms of the phenol groups by ca. 0.05 Å. However, the calculated Ln−N bond distances are in excellent agreement with the experimental values, as well as the calculated Ln−O_C bond distances (O_C = crown ether oxygen atoms), which are only slightly shorter than the experimental ones. The calculated mean ω angles are in the range 24.8−23.2°. Thus, the calculated structures show a larger deformation of the coordination polyhedron from a square antiprism (ideal value 45°) toward a square prism (ideal value 0°) than the experimental ones. The differences in the mean ω angles of the experimental and calculated structures are due to a somewhat different conformation of the pendant arms. The experimental C(1)−C(6)−C(7)−N(3) and C(36)−C(31)−C(30)−N(4) torsion angles [17.0(8)°] in $[Er(\mathbf{L^3}-2H)]^+$ show that the imine groups are not coplanar with the phenolate rings. However, the phenolate rings are nearly coplanar with the imine groups in the HF/3-21G* calculated structure of $[Er(\mathbf{L^3}-2H)]^+$ [C(1)−C(6)−C(7)−N(3) = −0.92°]. The $[Lu(\mathbf{L^3}-2H)]^+$ system was also fully optimized by using a better basis set for the ligand atoms (6-31G*). The corresponding calculated structure shows a mean ω angle of 24.7°, while the imine groups and the phenolate rings remain nearly coplanar [C(1)−C(6)−C(7)−N(3) = −2.29°]. Thus, the use of a better basis set for the ligand does not affect substantially the twist angle of the calculated structure. The $[Lu(\mathbf{L^3}-2H)]^+$ system was also fully optimized at the functional density theory (B3LYP) level. Comparison of the B3LYP/3-21G* and HF/3-21G* calculated structures (Table 4) shows that the inclusion of electron correlation causes negligible changes on the Lu(III) coordination environment, which is consistent with the ionic nature of the Ln−ligand bonds.[36] These results suggest that crystal packing forces in the solid state could be responsible for the different twist angles in the calculated and experimental structures.

The ^{13}C NMR shielding constants of the $[Lu(\mathbf{L^3}-2H)]^+$ complex were calculated on the in vacuo optimized structure by using the GIAO method. The main results of these calculations together with the experimental values are given in Table 2. Since the introduction of electron correlation effects has been demonstrated to be important for systems containing aromatic units,[33] the calculations of the NMR

Table 4. Values of the Main Geometrical Parameters of Experimental and Calculated Structures of $[Ln(\mathbf{L^3}-2H)]^+$ Complexes[a]

		exptl[b]	HF/3-21G*[c]	B3LYP/3-21G*[c]
Ce	Ho−N_A		2.761	
	Ho−N_I		2.634	
	Ho−O_P		2.324	
	Ho−O_C		2.548	
	ω[d]		24.8	
Sm	Ho−N_A		2.705	
	Ho−N_I		2.574	
	Ho−O_P		2.266	
	Ho−O_C		2.486	
	ω[d]		24.0	
Ho	Ho−N_A	2.654 (0.013)	2.653	
	Ho−N_I	2.510 (0.032)	2.517	
	Ho−O_P	2.157 (0.001)	2.205	
	Ho−O_C	2.444 (0.001)	2.425	
	ω[d]	33.9	23.5	
Er	Er−N_A	2.644 (0.000)	2.644	
	Er−N_I	2.501 (0.019)	2.507	
	Er−O_P	2.141 (0.002)	2.193	
	Er−O_C	2.437 (0.001)	2.415	
	ω[d]	34.1	23.5	
Tm	Tm−N_A		2.635	
	Tm−N_I		2.497	
	Tm−O_P		2.183	
	Tm−O_C		2.405	
	ω[d]		23.3	
Yb	Yb−N_A		2.626	
	Yb−N_I		2.488	
	Yb−O_P		2.172	
	Yb−O_C		2.394	
	ω[d]		23.2	
Lu	Lu−N_A		2.619	2.623
	Lu−N_I		2.481	2.453
	Lu−O_P		2.162	2.172
	Lu−O_C		2.386	2.392
	ω[d]		23.2	24.5

[a] Distances (Å), angles (deg); N_A = amine nitrogen atoms; N_I = imine nitrogen atoms; O_P = phenolate oxygen atoms; O_C = crown ether oxygen atoms. [b] The average values are reported with standard deviations in parentheses. [c] The two calculated distances between the lanthanide ion and the N_A, N_I, O_P, or O_C atoms differ by less than 0.001 Å. [d] Mean twist angle between the parallel planes defined by O(3), O(4), N(3), and N(4) (upper plane) and O(1), O(2), N(1), and N(2) (lower plane).

(30) Corey, E. J.; Bailar, J. C., Jr., *J. Am. Chem. Soc.* **1959**, *81*, 2620.
(31) Beattie, J. K. *Acc. Chem. Res.* **1971**, *4*, 253.
(32) Cosentino, U.; Villa, A.; Pitea, D.; Moro, G.; Barone, V. *J. Phys. Chem. B* **2000**, *104*, 8001.
(33) Platas-Iglesias, C.; Mato-Iglesias, M.; Djanashvili, K.; Muller, R. N.; Vander Elst, L.; Peters, J. A.; de Blas, A.; Rodríguez-Blas, T. *Chem Eur. J.* **2004**, *10*, 3579.
(34) Cosentino, U.; Villa, A.; Pitea, D.; Moro, G.; Barone, V.; Maiocchi, A. *J. Am. Chem. Soc.* **2002**, *124*, 4901.
(35) Quali, N.; Bocquet, B.; Rigault, S.; Morgantini, P.-Y.; Weber, J.; Piguet, C. *Inorg. Chem.* **2002**, *41*, 1436.
(36) Cosentino, U.; Moro, G.; Pitea, D.; Villa, A.; Fantucci, P. C.; Maiocchi, A.; Uggeri, F. *J. Phys. Chem. A* **1998**, *102*, 4606−4614.

shielding constants were performed at the B3LYP/6-31G** level. It has been demonstrated that the calculation of the NMR shielding constants using the 46+4f[14] core electron ECP of Dolg et al. provides inconsistent ^{13}C NMR chemical shifts.[34] Thus, we used the 46 core electron ECP by Stevens et al.,[21] which leaves the $4f^{14}$ electrons in the valence. In general, there is an excellent agreement between the experimental and calculated chemical shifts, as pointed out by the agreement factor obtained ($AF_j = 0.044$, eq 1),

$$AF_j = [\sum_i (\delta_{ij}^{exp} - \delta_{ij}^{cal})^2 / \sum_i (\delta_{ij}^{exp})^2]^{1/2} \quad (1)$$

where δ_{ij}^{exp} and δ_{ij}^{cal} are the experimental and calculated chemical shift values for a nucleus i of a given lanthanide complex j. These results point out that our ab initio calculations provide reasonably good models for the structure in solution of these complexes, and they confirm the assignment based on experimental NMR spectra.

In previous work we demonstrated that whereas receptor **L²** allows one to obtain stable complexes with the Ln(III) ions from La(III) to Ho(III), the larger receptor **L¹** (Chart 1) only forms stable complexes in acetonitrile solution with the three lightest lanthanide ions (La, Ce, and Pr), as a consequence of the combination of the relatively large ring size of the crown moiety and the presence of relatively rigid pendant arms. Likewise, herein we report that the smallest receptor **L³** is only able to form complexes of the heavier lanthanide ions (Ln = Ho−Lu). Aiming to understand the different coordination properties of the three receptors toward the Ln(III) ions, as well as to rationalize the potential selectivity shown by this family of receptors, we have also performed ab initio calculations on the $[Ln(\mathbf{L^1}-2H)]^+$ and $[Ln(\mathbf{L^2}-2H)]^+$ systems (Ln = Ce, Sm, Ho, Lu). A comparison of the calculated structures for the $[Ce(\mathbf{L^1}-2H)]^+$ and $[Ln(\mathbf{L^2}-2H)]^+$ (Ln = Ce, Sm) systems with the corresponding X-ray crystal structures previously reported[12,13] shows a reasonably good agreement between the experimental and calculated bond distances of the Ln(III) coordination sphere (Table S1, Supporting Information). For the $[Ln(\mathbf{L^3}-2H)]^+$ systems, the calculated bond distances between the metal ion and the ligand donor atoms decrease along the lanthanide series, as usually observed for Ln(III) complexes (Table 4, Figure 3). This results in a trend to higher stabilities across the lanthanide series that is common to the vast majority of lanthanide complexes.[37] However, a different situation occurs for the complexes of **L¹** and **L²** (Figure 3, see also Table S1, Supporting Information). For the complexes of **L¹** the distances between the lanthanide ion and the donor atoms of the pendant arms, as well as the distances between the metal ion and the oxygen atoms of the crown moiety, decrease along the lanthanide series. However, the distance between the lanthanide ion and the pivotal nitrogen atoms clearly increases across the series, which is in agreement with the experimental X-ray structures of the La(III) and Pr(III) complexes.[12] In the case of the $[Ln(\mathbf{L^2}-2H)]^+$ complexes a similar situation is observed; most of the Ln−donor distances decrease along the series. However, a dramatic increase in the distance between the Ln(III) ion and one of the oxygen atoms of the crown moiety

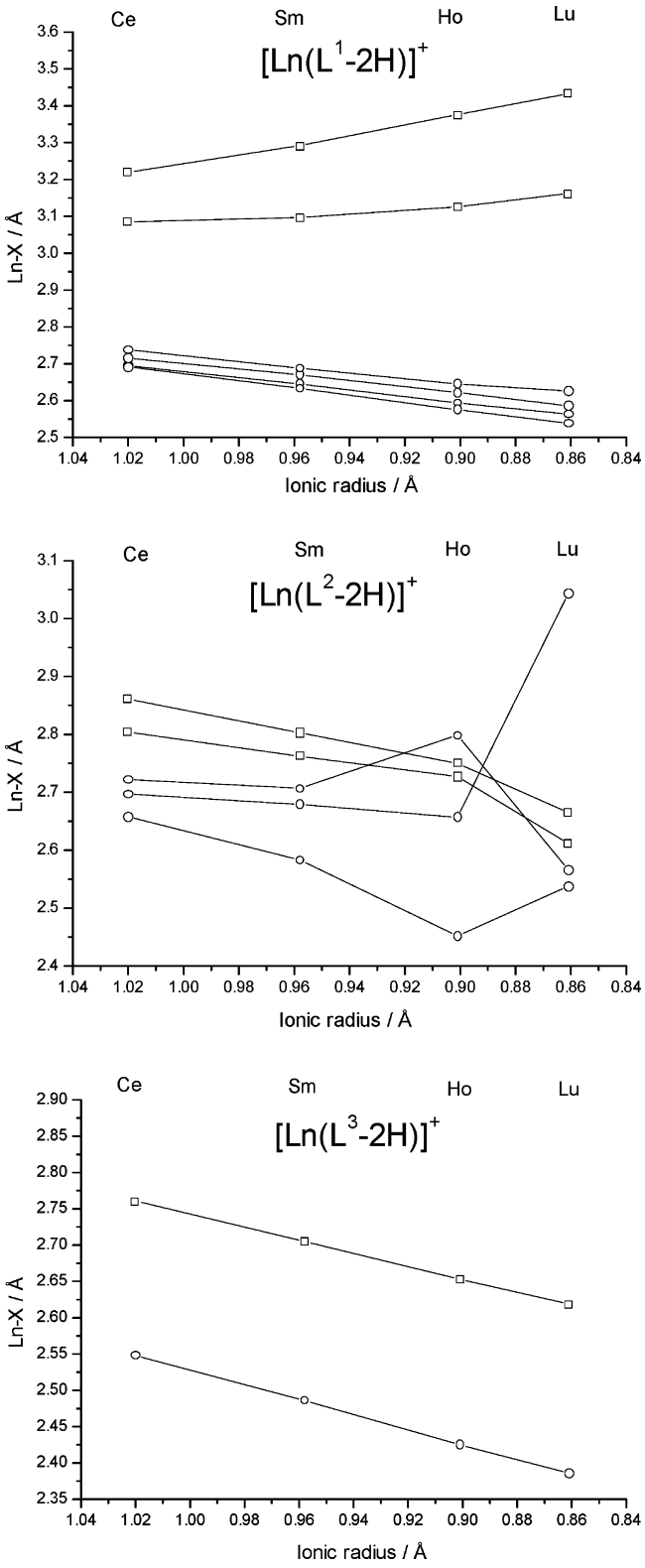

Figure 3. Ln−O_C (−○−) and Ln−N_A (−□−) bond distances calculated at the HF/3-21G* computational level for the $[Ln(\mathbf{L^1}-2H)]^+$, $[Ln(\mathbf{L^2}-2H)]^+$, and $[Ln(\mathbf{L^2}-2H)]^+$ complexes. N_A = amine nitrogen atoms; O_C = crown ether oxygen atoms.

(37) Piguet, C.; Edder, C.; Nozary, H.; Renaud, F.; Rigault, S.; Bünzli, J.-C. G. *J. Alloys Compd.* **2000**, *303−304*, 94.

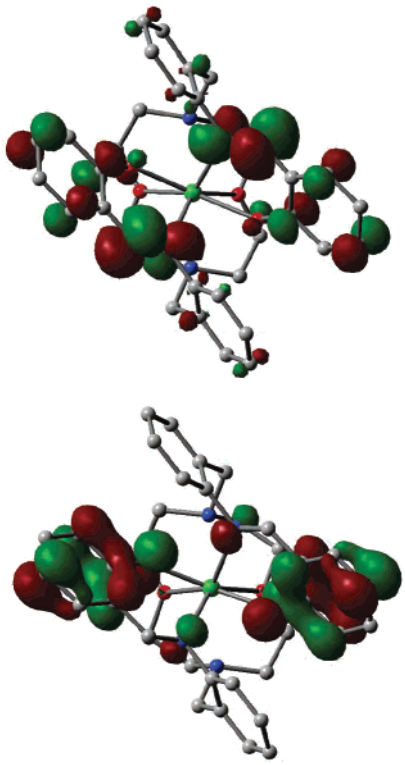

Figure 4. Calculated isosurface for the HOMO (bottom) and LUMO (top) in $[Lu(\mathbf{L^3}-2H)]^+$ at the B3LYP/3-21G* computational level. Hydrogen atoms are omitted for simplicity.

occurs between Ho(III) and Lu(III). As a consequence, while in the Ce(III), Sm(III), and Ho(III) complexes of $\mathbf{L^2}$ the metal ion is nonacoordinated, the metal ion in $[Lu(\mathbf{L^3}-2H)]^+$ is octacoordinated. Thus, it appears that, thanks to the variation of the ionic radii of the lanthanide ions, receptors $\mathbf{L^1}$ and $\mathbf{L^2}$ are specially adapted for the complexation of the lighter lanthanide ions.

Photophysical Properties. Electronic spectra of the Er(III), Yb(III), and Lu(III) complexes display three regions of absorption: two bands at ca. 272 and 230 nm corresponding to B and E_2 $\pi-\pi^*$ transitions of the substituted aromatic rings, respectively,[38] and a band centered around 369 nm typical of conjugated C═N chromophores (Figure S1, Supporting Information).[39] The latter assignment is in agreement with our electronic structure calculation performed on the $[Lu(\mathbf{L^3}-2H)]^+$ system at the B3LYP/3-21G* level. At the simplest conceptual level the band appearing at lowest energy in the absorption spectrum can be described as arising from the promotion of a single electron from the HOMO to the LUMO. For $[Lu(\mathbf{L^3}-2H)]^+$ the HOMO, which is derived from π(p) orbitals, shows the greatest electron density on the phenol rings and the imine nitrogen atoms (Figure 4). Using the approximate microsymmetry, C_2, the HOMO belongs to the B irreducible representation. Similarly, the LUMO is also derived mainly from π(p) orbitals of the phenol and imine groups and belongs to the B irreducible representation (Figure 4). Both the HOMO and LUMO are strictly ligand in character, with no participation of the metal. There appears to be substantial overlap between the HOMO and LUMO of $[Lu(\mathbf{L^3}-2H)]^+$, which should result in a rather intense electronic transition.

Table 5. Lanthanide Centered Photophysical Properties

compd	λ_{em}/nm	$\tau_{CH3CN}/\mu s$	$\tau_{CH3OH}/\mu s$	$\tau_{CD3OD}/\mu s$	q
Er	1530	0.78	0.42	0.78	*a*
Yb	980	4.34	2.92	4.65	0.15

[a] Values for *A* and *B* have not been established for erbium complexes, so calculation of the inner sphere hydration number is not possible.

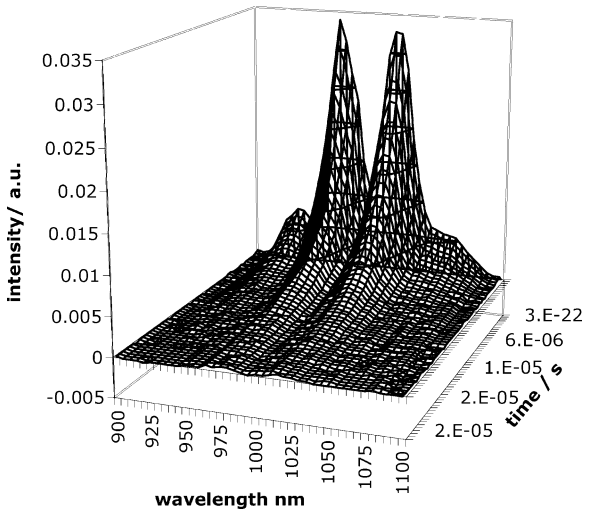

Figure 5. Time-resolved emission spectrum of the ytterbium complex at room temperature following excitation at 337 nm.

The fluorescence spectrum of the Lu(III) complex **5** recorded in acetonitrile solution (295 K) under excitation through the ligand bands (373 nm) exhibits a single band centered at ca. 465 nm assigned to emission from the $^1\pi\pi^*$ state. Attempts to locate the ligand triplet state from measurements at 77 K in an acetonitrile glass were unsuccessful. Taking into account that the position of the emission band corresponding to the $^1\pi\pi^*$ state is very similar for the complexes of $\mathbf{L^2}$ and $\mathbf{L^3}$, we estimate the 0-phonon transition of the ligand $^3\pi\pi^*$ state to lie at ca. 525 nm.[13] The relatively low energy of the ligand $^3\pi\pi^*$ state makes $\mathbf{L^3}$ especially suited for the sensitization of Yb(III) or Er(III) ions, which emit in the near-infrared.

Luminescence studies were also carried out on the ytterbium and erbium complexes. Their luminescence lifetimes in acetonitrile and methanolic media are shown in Table 5, while Figures 5 and 6 show the time-resolved emission spectra for the ytterbium and erbium complexes, respectively. In all cases, the photophysical properties of the complexes in acetonitrile approximated those measured in CD_3OD. By contrast, the luminescence in CH_3OH was less intense and shorter-lived as a result of more effective nonradiative quenching of the excited states in the presence of O−H oscillators.

Luminescence from a wide variety of ytterbium complexes has been studied in great detail in recent years, and it is possible to apply the lessons learned from these studies to our system.[40] The luminescence lifetimes in methanolic solution can be used to obtain the inner sphere

(38) Silverstein, R. M.; Bassler, C. *Spectrometric Identification of Organic Compounds*; Wiley Int.: New York, 1967.
(39) Aruna, V. A. J.; Alexander,V. *Chem. Soc., Dalton Trans.* **1996**, 1867.

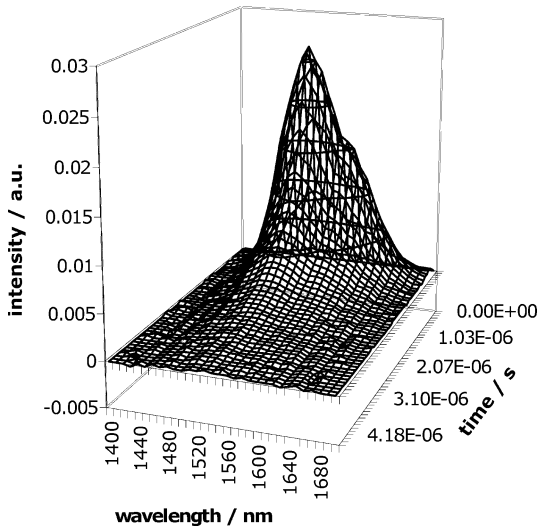

Figure 6. Time-resolved emission spectrum of the erbium complex at room temperature following excitation at 337 nm.

hydration number, q, using eq 2,

$$q = A(1/\tau_{CH3OH} - 1/\tau_{CD3OD} - B) \qquad (2)$$

where A and B are constants for a given lanthanide and τ_{CH3OD} and τ_{CD3OD} are the luminescence lifetimes in CH_3OH and CD_3OD, respectively.[41] For ytterbium in methanolic solution, A and B have been found to be 2.0 μs^{-1} and 0.05 μs, respectively. Using these values we obtain a calculated inner sphere of 0.15, suggesting that there are no bound solvent molecules in the inner coordination sphere. This suggests that complexes derived from this ligand are ideally suited for use as luminescent tags for time gated imaging,[42,43] since nonradiative quenching by solvent is minimized.

It is worth noting that energy transfer from the ligand chromophore appears to be very rapid and is complete within the envelope of the laser pulse. Such rapid energy transfer may be consistent with efficient phonon assisted energy transfer through the vibrational overtones of the ligand and the solvent manifold, or it may result from mediation of energy transfer by a double electron transfer mechanism (which is thermodynamically feasible for phenolate chromophores coordinated to the metal center).[44]

Luminescence from erbium complexes is less well understood. The erbium complex studied here is rather unusual, in that it was possible to record luminescence spectra and lifetimes in protic media. Quenching by O−H oscillators is normally so efficient that the luminescence in protic media is quenched almost completely, while the signals observed are too weak and short-lived to measure. In this case, long-lived emission is observed centered around 1530 nm in CH_3OH, suggesting that the solution-state structure resembles the crystal structure described above and that solvent is excluded from the inner sphere. The much longer lifetimes observed in deuterated solvent and acetonitrile suggest that outer sphere O−H quenching is much more effective for erbium than for ytterbium.

Conclusions

In its di-deprotonated form, the Schiff-base bibracchial lariat ether *N*,*N*′-bis(2-salicylaldiminobenzyl)-4,10-diaza-12-crown-4 forms complexes with the heaviest Ln(III) ions (Ln = Ho−Lu). The X-ray crystal structures of the Ho(III) (**1**) and Er(III) (**2**) complexes show the metal ion being directly bound to the eight donor atoms of the macrocyclic ligand. Attempts to isolate complexes of the lightest members of the lanthanide series were unsuccessful, which suggests a certain degree of selectivity of $\mathbf{L^3}$ toward the heaviest Ln(III) ions. This one can be rationalized on the basis of theoretical calculations performed in vacuo at the HF level. For the $[Ln(\mathbf{L^3}-2H)]^+$ systems, the calculated bond distances between the metal ion and the coordinated ligand atoms decrease along the lanthanide series, as usually observed for Ln(III) complexes; however, for the related systems $[Ln(\mathbf{L^1}-2H)]^+$ and $[Ln(\mathbf{L^2}-2H)]^+$ our ab initio calculations provide geometries in which some of the bond distances of the metal coordination environment increase across the lanthanide series. Thus, thanks to the variation of the ionic radii of the lanthanide ion receptors $\mathbf{L^1}$ and $\mathbf{L^2}$ are specially adapted for the complexation of the lighter lanthanide ions. The results presented here demonstrate that it should be possible to design rigid receptors selective for a particular group of Ln(III) ions.

On the other hand, the luminescence properties of the $[Lu(\mathbf{L^3}-2H)]^+$ complexes here presented make them ideally suited for use as luminescent tags, and suggest that $q = 0$ complexes of erbium may, after all, be useful as luminescent tags in protic media. We are currently investigating ways to improve the solubility of the ligands and complexes in aqueous media.

Acknowledgment. M.G.-L., C.P.-I., F.A., A.d.B., and T.R.-B. thank Ministerio de Ciencia y Tecnología and FEDER (BQU2001-0796), and Xunta de Galicia (PGIDIT02-PXIC10301PN) for financial support. Likewise, the support and sponsorship arranged by COST Action D18 "Lanthanide Chemistry for Diagnosis and Therapy" is kindly acknowledged. The authors are also indebted to the Centro de Supercomputación de Galicia (CESGA) for providing the computer facilities.

Supporting Information Available: X-ray crystallographic files, in CIF format, for **1** and **2**, electronic absorption spectrum of compound **4** (Figure S1), Table S1 listing bond distances of the metal coordination environment in experimental and calculated structures of $[Ln(\mathbf{L^1}-2H)]^+$ and $[Ln(\mathbf{L^2}-2H)]^+$ complexes, and in vacuo optimized Cartesian coordinates (Å) of $[Ln(\mathbf{L^1}-2H)]^+$, $[Ln(\mathbf{L^2}-2H)]^+$, and $[Ln(\mathbf{L^2}-2H)]^+$complexes. This material is available free of charge via the Internet at http://pubs.acs.org.

IC048172A

(40) Faulkner, S.; Matthews, J. L. In *Comprehensive Coordination Chemistry II*; Ward, M. D., Ed.; Elsevier: Oxford, 2004; p 913.
(41) Beeby, A.; Clarkson, I. M.; Dickins, R. S.; Faulkner, S.; Parker, D.; Royle, L.; de Sousa, A. S.; Williams, J. A. G.; Woods, M. *J. Chem. Soc, Perkin Trans. 2* **1999**, 493.
(42) Beeby, A.; Botchway, S. W.; Clarkson, I. M.; Faulkner, S.; Parker, A. W.; Parker, D.; Williams, J. A. G. *J. Photochem. Photobiol., B* **2000**, *57*, 83.
(43) Wiebel, N.; Charbonniere, L. J.; Guardigli, M.; Roda, A.; Ziessel, R. *J. Am. Chem. Soc.* **2004**, *126*, 4888.
(44) Beeby, A.; Faulkner, S.; Williams, J. A. G. *J. Chem. Soc., Dalton Trans.* **2002**, 1918.